Computers and Geotechnics 49 (2013) 7–17

Contents lists available at SciVerse ScienceDirect

Computers and Geotechnics

journal homepage: www.elsevier.com/locate/compgeo

A finite element formulation of gradient-based plasticity for porous media with C1 interpolation of internal variables

Javier L. Mroginski [a,*], Guillermo Etse [b]

[a] Applied Mechanical Dept., Universidad Nacional del Nordeste, Las Heras 727, Resistencia, Chaco, Argentina
[b] CONICET and Faculty for Exact Sciences & Technology, Universidad Nacional de Tucumán, Maipu 780, 4000 Tucumán, Argentina

ARTICLE INFO

Article history:
Received 1 March 2012
Received in revised form 26 October 2012
Accepted 5 November 2012
Available online 7 December 2012

Keywords:
Gradient theory
Porous media
C_1-continuous FE
Thermodynamic consistent

ABSTRACT

In this paper a new finite element formulation for numerical analysis of diffused and localized failure behavior of saturated and partially saturated gradient poroplastic materials is proposed. The new finite element includes interpolation functions of first order (C_1) for the internal variables field while classical C_0 interpolation functions for the kinematic fields and pore pressure. This finite element formulation is compatible with a thermodynamically consistent gradient poroplastic theory previously proposed by the authors. In this material theory the internal variables are the only ones of non-local character. To verify the numerical efficiency of the proposed finite element formulation, the non-local gradient poroplastic constitutive theory is combined with the modified Cam Clay model for partially saturated continua. Thereby, the volumetric strain of the solid skeleton and the plastic porosity are the internal variables of the constitutive theory. The numerical results in this paper demonstrate the capabilities of the proposed finite element formulation to capture diffuse and localized failure modes of boundary value problems of porous media, depending on the acting confining pressure and on the material saturation degree.

1. Introduction

Gradient-based constitutive formulations are widely used in mechanical modeling of strain softening materials. Since the pioneer work by Vardoulakis and Aifantis [1], the strain gradient material theory gained relevant echo in the international scientific community. Amount others, proposals [2–7] demonstrate both the extensive use of gradient theory in solid materials and its effectiveness to limit the severe mesh size dependency of the so-called smeared crack approach.

From the predictive capabilities stand point, strain gradient based constitutive models lead to appreciable diffusions of the failure modes. This is due to the intrinsic well-posedness of the governing equations in case of gradient theory that are able to suppress the loss of strong ellipticity in the form of discontinuous bifurcation of the related local constitutive equations. Nevertheless, the strong diffusion of failure modes predicted by gradient-based models is a relevant disadvantage of this non-local material theory in case of failure behavior of cohesive-frictional materials like rocks, concretes and partial saturated soils, when loaded in the low confinement or tensile regimes [8,9]. In these cases the shortcomings of classical gradient constitutive models to reproduce the localized failure modes of quasi-brittle materials strongly affect the numerical prediction accuracy despite the mesh objective solutions their provide.

The constitutive theory for partially saturated porous media recently proposed by Mroginski et al. [10] is oriented to solve this deficiency. By considering a selective level of gradient non-locality this material theory is able to reproduce diffuse and localized failure modes of partially saturated porous media.

From the finite element (FE) stand point, strain gradient constitutive formulations require special provisions for the approximation of the Laplacian to the plastic multiplier in the element domains and on their boundaries. Pioneer contributions in FE technology related to gradient formulations in non-porous media are [11,12] who proposed C_1 continuity elements to approximate the non-local strain gradient fields, and [13], who proposed a four node FE with one integration point for large strain and strain gradients. FE formulations with C_0 continuity based approximation fields for gradient constitutive models of non-porous media were proposed in [14–18]. The proposal by De Borst and Pamin [14] considers penalty functions to avoid additional iterations in the solution procedure for the non-local gradient strain fields. This FE formulation includes rotation as nodal variable. It should be noted that the overall numerical performance of this FE is not efficient, as can be observed in [19]. In the others C_0-continuous FE for gradient-based continua [6,20], the non-local effects are considered to be restricted to the internal variables while their numerical approaches

* Corresponding author.
E-mail addresses: javierm@ing.unne.edu.ar (J.L. Mroginski), getse@herrera.unt.edu.ar (G. Etse).

0266-352X/$ - see front matter © 2012 Elsevier Ltd. All rights reserved.
http://dx.doi.org/10.1016/j.compgeo.2012.11.003

for the variable fields involves additional iterative procedures to solve for the plastic multiplier Laplacian.

Regarding the strain localization problem in saturated soils Stankiewicz and Pamin developed a FE formulation for non-local Cam Clay model based on the strain gradient theory by [11]. It considers, on the one hand, a one-phase approach under fully drained and undrained hydraulic condition [21,22] while, on the other hand, a two-phase approach to take into account the permeability and, therefore, the stabilizing role of the fluid phase [23]. Despite the similarities in the numerical approach between present gradient plasticity formulation and those proposed by Stankiewicz and Pamin [21,22] there are two important differences. On the one hand, in this proposal the internal variables are the only ones of non-local character while in classical formulations of gradient plasticity [11,12,20,21] the non-local variables are the strains. On the other hand, in present gradient-based poroplastic formulation there are two characteristic lengths involved, one for the skeleton and the other for the porous phase.

In conclusion: despite the considerable progress made in FE formulation for gradient based materials, there is still a need of efficient FE technologies for thermodynamically consistent partially saturated porous media, in which the kinematic fields of the skeleton interact with the hydraulic and pressure fields of the porous phase.

In this work a new C_1 continuity based FE formulation is proposed for gradient-based constitutive formulation of saturated and partially saturated porous media with the capacity to reproduce both localized and diffuse failure modes that characterized quasi-brittle materials like concrete and soils. A distinguish aspect of this FE formulation is the inclusion of interpolation functions of first order continuity (C_1) only for the internal variables field while the kinematic fields remain with the classical C_0-continuous interpolation functions. This FE technology is particularly appropriated to be used with the thermodynamically consistent non-local gradient theory by the authors in [10], and involve one single iteration loop for the plastic multiplier an its Laplacian. This strongly reduces the computational time. Similarly to [6,20] present FE formulation considers gradient material models with internal variables being the only ones of non-local character. This reduces the involved complexity of the FE formulation.

After a brief summarization of the main features of the thermodynamic material theory for porous materials [10] in Sections 2 and 3, the paper focuses in the formulation of the proposed four node FE for gradient-based porous media in Section 4. In Section 5, the numerical analyses illustrate the predictive capabilities of the proposed FE in combination with the considered constitutive theory to reproduce the different failure modes of partially saturated porous materials depending on the stress state and hydraulic conditions.

2. No local gradient plasticity for porous media

In this section the thermodynamically consistent gradient plasticity theory for porous media by Mroginski et al. [10] is summarized.

2.1. Dissipative stress in porous media

Based on previous studies developed by [24,25], it is assumed that arbitrary thermodynamic states of the dissipative material during isothermal processes are completely determined by the elastic strain tensor $\boldsymbol{\varepsilon}^e = \boldsymbol{\varepsilon} - \boldsymbol{\varepsilon}^p$, and the internal variables q_α with $\alpha = s, p$ for solid or porous phase, respectively, which are considered here as scalars. When considering poroplastic materials the elastic variation of fluid mass content $m^e = m - m^p$ needs also to be included as a thermodynamic argument of the free energy, see [25]. It is further assumed that internal variables are the only one of non-local character and, therefore, the spacial gradients ∇q_α are also included in the formulation, see [10,26,27]. The extension to more than two scalar internal variables is straightforward. Hence, both q_α and ∇q_α together with $\boldsymbol{\varepsilon}^e$ and m^e will appear as arguments in the Helmholtzs free energy

$$\Psi = \Psi(\boldsymbol{\varepsilon}^e, m^e, q_\alpha, \nabla q_\alpha) \tag{1}$$

while the Clausius–Duhem inequality (CDI) results

$$\int_\Omega \frac{1}{\theta}\left[(\boldsymbol{\sigma} - \rho\partial_{\boldsymbol{\varepsilon}^e}\Psi) : \dot{\boldsymbol{\varepsilon}} + (p - \rho\partial_{m^e}\Psi)\dot{m} + \rho\partial_{\boldsymbol{\varepsilon}^e}\Psi : \dot{\boldsymbol{\varepsilon}}^p + \rho\partial_{m^e}\Psi\dot{m}^p - \sum_\alpha \rho\partial_{q_\alpha}\Psi\dot{q}_\alpha - \sum_\alpha \rho\partial_{\nabla q_\alpha}\Psi\nabla\dot{q}_\alpha\right] \mathrm{d}\Omega \geqslant 0 \tag{2}$$

where $\boldsymbol{\sigma}$ is the stress tensor, p the pore pressure, ρ the mass density, and the compact notation $\partial_x(\bullet) = \frac{\partial(\bullet)}{\partial x}$ was adopted for partial derivatives. By integrating the gradient term by parts and using de Divergence Theorem results

$$\int_\Omega \frac{1}{\theta}[(\boldsymbol{\sigma} - \rho\partial_{\boldsymbol{\varepsilon}^e}\Psi) : \dot{\boldsymbol{\varepsilon}} + (p - \rho\partial_{m^e}\Psi)\dot{m} + \rho\partial_{\boldsymbol{\varepsilon}^e}\Psi : \dot{\boldsymbol{\varepsilon}}^p + \rho\partial_{m^e}\Psi\dot{m}^p + \sum_\alpha Q_\alpha\dot{q}_\alpha]\mathrm{d}\Omega + \int_{\partial\Omega}\sum_\alpha Q_\alpha^{(b)}\dot{q}_\alpha \,\mathrm{d}\partial\Omega \geqslant 0 \tag{3}$$

where the dissipative stresses Q_α and $Q_\alpha^{(b)}$ are defined as

$$Q_\alpha = -\rho\partial_{q_\alpha}\Psi - \nabla\cdot(\rho\partial_{\nabla q_\alpha}\Psi) \quad \text{in } \Omega \tag{4}$$

$$Q_\alpha^{(b)} = -\rho\partial_{\nabla q_\alpha}\Psi\mathbf{n} \quad \text{on } \partial\Omega \tag{5}$$

In the standard local theory it is postulated that the inequality (3) must hold for any choice of domain and for any independent thermodynamic process. As a result, Colemans equation are formally obtained like in local plasticity

$$\boldsymbol{\sigma} = \rho\partial_{\boldsymbol{\varepsilon}^e}\Psi \tag{6}$$

$$p = \rho\partial_{m^e}\Psi \tag{7}$$

$$\mathfrak{D} = \boldsymbol{\sigma} : \boldsymbol{\varepsilon}^e + p\dot{m}^p + \sum_\alpha Q_\alpha\dot{q}_\alpha \geqslant 0 \quad \text{in } \Omega \tag{8}$$

$$\mathfrak{D}^{(b)} = \sum_\alpha Q_\alpha^{(b)}\dot{q}_\alpha \geqslant 0 \quad \text{on } \partial\Omega \tag{9}$$

In case $p = 0$, above equations take similar form to the formulations by [26,27] for non-porous media. Also, from Eqs. (8) and (9) it can be concluded that the dissipative stress Q_α can be decomposed into the local and non-local components

$$Q_\alpha = Q_\alpha^{loc} + Q_\alpha^{nloc} \tag{10}$$

with

$$Q_\alpha^{loc} = -\rho\partial_{q_\alpha}\Psi \tag{11}$$

$$Q_\alpha^{nloc} = -\rho\nabla\cdot(\partial_{\nabla q_\alpha}\Psi) \tag{12}$$

2.2. Thermodynamically consistent gradient-based elastoplastic constitutive relationship

Following [26,27], the free energy density of non-local gradient poroplastic materials can be additively expressed as

$$\Psi(\boldsymbol{\varepsilon}^e, m^e, q_\alpha, \nabla q_\alpha) = \Psi^e(\boldsymbol{\varepsilon}^e, m^e) + \Psi^{p,loc}(q_\alpha) + \Psi^{p,nloc}(\nabla q_\alpha) \tag{13}$$

with the elastic energy density,

$$\rho\Psi^e = \boldsymbol{\sigma}^0 : \boldsymbol{\varepsilon}^e + p^0 m^e + \frac{1}{2}\boldsymbol{\varepsilon}^e : \mathbf{C}^0 : \boldsymbol{\varepsilon}^e + \frac{1}{2}M(\mathbf{B} : \boldsymbol{\varepsilon}^e - m^e)^2 \tag{14}$$

and the local and non-local plastic energy densities $\Psi^{p,loc}$ and $\Psi^{p,nloc}$, respectively, expressed in terms of the internal variables q_α and their gradients ∇q_α.

2.3. Non-local plastic flow rule

The hardening rule and the non-associated flows of both plastic strains and fluid mass content are formulated in rate form as

$$\dot{\boldsymbol{\varepsilon}}^p = \dot\lambda \partial_{\boldsymbol{\sigma}} \Phi^* = \dot\lambda \mathbf{m}_\sigma; \quad \dot m^p = \dot\lambda \partial_p \Phi^* = \dot\lambda \mathrm{m}_p; \\ \dot q_\alpha = \dot\lambda \partial_{Q_\alpha} \Phi^* = \dot\lambda \mathrm{m}_{Q_\alpha} \tag{15}$$

being Φ^* the plastic dissipative potential.

To complete problem formulation in Ω, the Kuhn–Tucker complementary conditions are introduced

$$\dot\lambda \geqslant 0; \quad \Phi(\boldsymbol{\sigma}, p, Q_\alpha) \leqslant 0; \quad \dot\lambda \Phi(\boldsymbol{\sigma}, p, Q_\alpha) = 0 \tag{16}$$

In the undrained condition, when the additive decomposition of the free energy potential in Eq. (13) and the flow rules of Eq. (15) are considered, the following expressions of $\dot{\boldsymbol{\sigma}}$ and $\dot p$ are obtained

$$\dot{\boldsymbol{\sigma}} = \mathbf{C} : \dot{\boldsymbol{\varepsilon}} - \dot\lambda \mathbf{C} : \mathbf{m}_\sigma - M\mathbf{B}\dot m + \dot\lambda M \mathbf{B} m_p \tag{17}$$

$$\dot p = -M\mathbf{B} : \dot{\boldsymbol{\varepsilon}} + \dot\lambda M \mathbf{B} : \mathbf{m}_\sigma + M\dot m - \dot\lambda M m_p \tag{18}$$

being M the Biot's module, $\mathbf{B} = b\mathbf{I}$ with b the Biot coefficient and $\mathbf{I}$ the second-order unit tensor, and $\mathbf{C} = \mathbf{C}^0 + M\mathbf{B} \otimes \mathbf{B}$. Thereby is $\mathbf{C}^0$ the fourth-order elastic tensor.

After multiplying Eq. (18) by $\mathbf{B}$ and combining with Eq. (17), a more suitable expression of the rate of the stress tensor for drained condition is achieved

$$\dot{\boldsymbol{\sigma}} = \mathbf{C}^0 : \dot{\boldsymbol{\varepsilon}} - \mathbf{B}\dot p - \dot\lambda \mathbf{C}^0 : \mathbf{m}_\sigma \tag{19}$$

while the evolution laws of the local and non-local dissipative stresses in Eq. (10) result

$$\dot Q_\alpha^{loc} = -\dot\lambda H_\alpha^{loc} \mathbf{m}_Q \tag{20}$$

$$\dot Q_\alpha^{nloc} = l_\alpha^2 \nabla \cdot \left(\mathbf{H}_\alpha^{nloc} \nabla \dot\lambda \mathrm{m}_{Q_\alpha} + \dot\lambda \mathbf{H}_\alpha^{nloc} \cdot \nabla Q_\alpha \mathbf{m}_Q^2 \right) \tag{21}$$

where $\mathbf{m}_Q^2 = \partial^2 \Phi^* / \partial Q^2$. Thereby, the local hardening/softening module H_α^{loc} have been introduced as well as the non-local hardening/softening tensor $\mathbf{H}_\alpha^{nloc}$ as defined in [26]

$$H_\alpha^{loc} = \rho \frac{\partial^2 \Psi^{p,loc}}{\partial q_\alpha^2}, \quad \mathbf{H}_\alpha^{nloc} = \rho \frac{1}{l_\alpha^2} \frac{\partial^2 \Psi^{p,nloc}}{\partial \nabla q_\alpha \partial \nabla q_\alpha} \tag{22}$$

with $\mathbf{H}_\alpha^{nloc}$ a second-order positive defined tensor. For the characteristic length l_α three alternative definitions can be given, see [19,28,29]. On the one hand, it can be defined as a convenient dimensional parameter so as H_α^{loc} and $\mathbf{H}_\alpha^{nloc}$ will get the same dimension. On the other hand, l_α can be interpreted as an artificial numerical stabilization mechanism for the non-local theory. Alternatively, as a physical entity that characterizes the material microstructure. In this last case, and for calibration purpose, specific numerical analysis on the representative volume element (RVE) need to be performed at micro scale level.

3. Modified Cam Clay constitutive model for gradient plasticity

The modified Cam Clay plasticity model was originally proposed by [30] for normally consolidated clays. Due to its good predictions of consolidated clay mechanical behavior and to the reduced number of involved parameters the Cam Clay material theory has been extended to a wide range of soils including unsaturated ones [31,32] and cyclic external actions [33].

The yield function is defined by

$$\Phi(\sigma', \tau, Q_\alpha) = \left(\sigma' + \frac{\tau^2}{m^2 \sigma'} \right) - Q_\alpha \tag{23}$$

where $\sigma' = I_1/3 - \beta p$ is the effective hydrostatic stress, $\tau = \sqrt{3J_2}$ the shear stress, m the Critical State Line (CSL) slope and Q_α the thermodynamically consistent dissipative stress equivalent to the preconsolidation pressure p_{co}. Also I_1 and J_2 are the first and second invariants of the stress tensor and the deviator tensor, respectively.

To avoid overestimation of the volumetric compressibility coefficient K_0 by the conventional critical state model a non-associated flow rule was introduced by [21,34]. Thereby, the following plastic potential is proposed

$$\Phi^*(\sigma', \tau, Q_\alpha) = \eta(\sigma'^2 - \sigma' Q_\alpha) + \left(\frac{\tau}{m} \right)^2 \tag{24}$$

$\eta$is a coefficient that limits the influence of the volumetric pressure during softening regime.

The thermodynamic consistency is achieved by assuming the following expression for the dissipative part of the free energy in Eq. (13)

$$\rho \Psi^p(\varepsilon^p, \nabla \varepsilon^p) = \rho \Psi^{p,loc}(\varepsilon^p) + \rho \Psi^{p,nloc}(\nabla \varepsilon^p) \\ = -\frac{1}{\chi} p_{co}^0 \exp(\chi \varepsilon^p) - \frac{1}{2} l_\alpha^2 \mathbf{H}^{nloc} \nabla \cdot \nabla \varepsilon^p \tag{25}$$

where the coefficient χ is defined by

$$\chi = -\frac{\beta(1 + e_0)}{\gamma - \kappa} \tag{26}$$

being β an adjustment coefficient (assumed $\beta = 1$ in this work), e_0 the initial void ratio, γ a hardening parameter and κ the swelling index (obtained from the odometry test).

The volumetric plastic strain of the continuous porous media, ε^p, is expressed as a function of the internal variables in order to describe the plastic evolutions of the porous and solid phases, in terms of the plastic porosity ϕ^p and the volumetric plastic strain of soil grain ε_s^p, respectively [25]

$$\varepsilon^p = \phi^p + (1 - \phi_0)\varepsilon_s^p \tag{27}$$

From Eqs. (11) and (12) the following expressions for local and non-local dissipative stresses are obtained

$$Q_\alpha^{loc}(\varepsilon^p) = -\rho \partial_{\varepsilon^p} \Psi = p_{co}^0 \exp\left(\chi \left(\phi^p + (1 - \phi_0)\varepsilon_s^p \right) \right) \tag{28}$$

$$Q_\alpha^{nloc}(\nabla \varepsilon^p) = -\rho \nabla \cdot (\partial_{\nabla \varepsilon^p} \Psi) = l_s^2 \mathbf{H}_s^{nloc} \nabla^2 \varepsilon_s^p + l_p^2 \mathbf{H}_p^{nloc} \nabla^2 \phi^p \tag{29}$$

where l_s and l_p are the internal characteristic lengths for solid skeleton and porous phase, respectively.

In the present formulation the combination between both internal characteristic lengths, the one for the solid skeleton l_s and the other for the porous phase l_p, defines the width of the shear band where the degradation of the material located in between active cracks occurs.

In quasi-brittle porous materials like soils and concrete the strength degradation process in the post-peak regime may be controlled by two independent variables, the acting confining pressure during softening process and the pore water content. This dependence can be mathematically described though the expression defining the internal characteristic length.

From Vrech and Etse [27] the internal characteristic length for solid phase takes the following form (see Fig. 1)

$$l_s(\sigma') = \begin{cases} 0 & \text{for } \sigma' \leqslant 0 \\ \frac{l_{s,m}}{2} \left[1 + \sin\left(\frac{\pi}{Q_\alpha/2} \sigma' - \frac{\pi}{2} \right) \right] & \text{for } 0 < \sigma' \leqslant Q_\alpha/2 \\ l_{s,m} & \text{for } \sigma' > Q_\alpha/2 \end{cases} \tag{30}$$

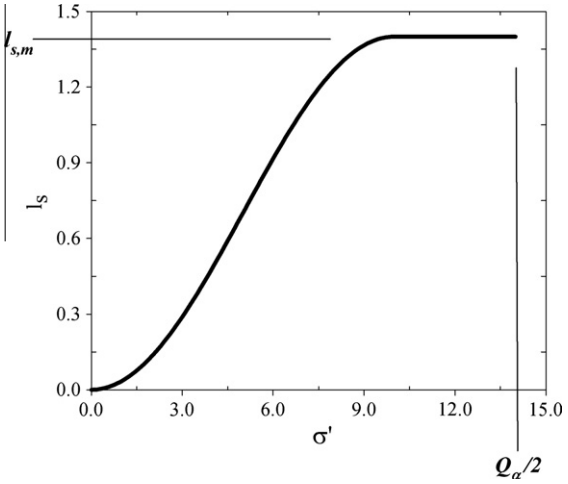

Fig. 1. Internal characteristic length of solid phase vs. σ'.

The internal characteristic length of the porous phase is governed by the saturation degree S_w or, indirectly by the acting pore pressure. As the soil specimen dries, l_p tends to zero, and brittle failure behavior is expected. On the other hand, when the water content increases, l_p tends to its maximum value $l_{p,m}$, and ductile failure response is expected.

The saturation degree of the porous medium can be associated with the pore pressure (or suction) by a logarithmic expression [35,36] which depends on different experimental coefficients, i.e. the soil–water characteristic curve. Another option to describe the relationship between the saturation degree and the pore pressure is an hyperbolic function as proposed by [37]. This function can be easily inverted, while no further algorithm for the solution of the root is required. Then,

$$p = \frac{1}{2\,b}\ln\left(\frac{a+S_w}{a-S_w}\right) \tag{31}$$

being a and b two setting parameters. In Fig. 2a Eq. (31) is plotted, being p_{100} the pore water pressure corresponding to a fully saturated specimen.

Thus, the following expression for the internal characteristic length of the porous phase is proposed (see Fig. 2b)

$$l_p(p) = \begin{cases} 0 & \text{for } p \leqslant 0 \\ a\; l_{p,m}\tanh(b\; l_p) & \text{for } 0 < p \leqslant p_{100} \end{cases} \tag{32}$$

4. Finite element formulation

In this section the finite element formulation is presented together with its iterative algorithm to solve the field variable increments of boundary value problems (BVP) related to gradient-based poroplastic media. The solution of the BVP should enforce the equilibrium, fluid mass balance and yield conditions, at the end of each increment by considering the hydro-mechanical coupling.

4.1. Incremental formulation

At the end of the $j+1$ iteration of current load step, the incremental equilibrium condition, the fluid mass balance, and the yield condition are studied in a weak form as follows,

$$\int_\Omega \delta\boldsymbol{\varepsilon}^T : \boldsymbol{\sigma}_{j+1}\; \mathrm{d}\Omega - \int_{\partial\Omega} \delta\mathbf{u}^T\mathbf{t}_{j+1}\; \mathrm{d}\partial\Omega = 0 \tag{33}$$

$$\int_\Omega \delta p\dot{m}_{j+1}\; \mathrm{d}\Omega - \int_\Omega \nabla\delta p\cdot\mathbf{w}_{j+1}\; \mathrm{d}\Omega + \int_{\partial\Omega}\delta p\mathbf{w}_{j+1}\cdot\mathbf{n}\; \mathrm{d}\partial\Omega = 0 \tag{34}$$

$$\int_\Omega \delta\lambda\; \Phi(\boldsymbol{\sigma},p,Q_\alpha)|_{j+1}\; \mathrm{d}\Omega = 0 \tag{35}$$

being $\mathbf{w} = -\mathbf{k}\cdot\nabla p$ the generalized Darcy's law for porous media [25,36,38].

Differently to the local plasticity algorithm, Eq. (35) is not satisfied strictly but in a weak form. Furthermore, it is only fulfilled when the convergence is reached and not necessarily during the iterative process.

Considering the decomposition of stress tensor in the $j+1$ iteration as $\boldsymbol{\sigma}_{j+1} = \boldsymbol{\sigma}_j + \Delta\boldsymbol{\sigma}$, where Δ the increment of the field variable at the end of iteration $j+1$ and iteration j, and replacing in Eq. (33) result

$$\int_\Omega \delta\boldsymbol{\varepsilon}^T : \Delta\boldsymbol{\sigma}\; \mathrm{d}\Omega = \int_{\partial\Omega}\delta\mathbf{u}^T\mathbf{t}_{j+1}\; \mathrm{d}\partial\Omega - \int_\Omega \delta\boldsymbol{\varepsilon}^T : \boldsymbol{\sigma}_j\; \mathrm{d}\Omega \tag{36}$$

replacing $\Delta\boldsymbol{\sigma}$ in the last equation by the linearized form of Eq. (19),

$$\int_\Omega \delta\boldsymbol{\varepsilon}^T : (\mathbf{C}^0 : \Delta\boldsymbol{\varepsilon} - \mathbf{B}\Delta p - \mathbf{C}^0 : \mathbf{m}_\sigma\Delta\lambda)\mathrm{d}\Omega = \int_{\partial\Omega}\delta\mathbf{u}^T\mathbf{t}_{j+1}\mathrm{d}\partial\Omega - \int_\Omega \delta\boldsymbol{\varepsilon}^T : \boldsymbol{\sigma}_j\mathrm{d}\Omega \tag{37}$$

It can be observed that Eq. (37) is very similar to the incremental equilibrium condition of classical plasticity as it does not include an explicit dependence on the Laplacian of the plastic multiplier.

Considering the incremental decomposition of the infiltration vector $\mathbf{w}_{j+1} = \mathbf{w}_j + \Delta\mathbf{w}_{j+1}$ and the rate of the fluid mass content $\dot{m}$

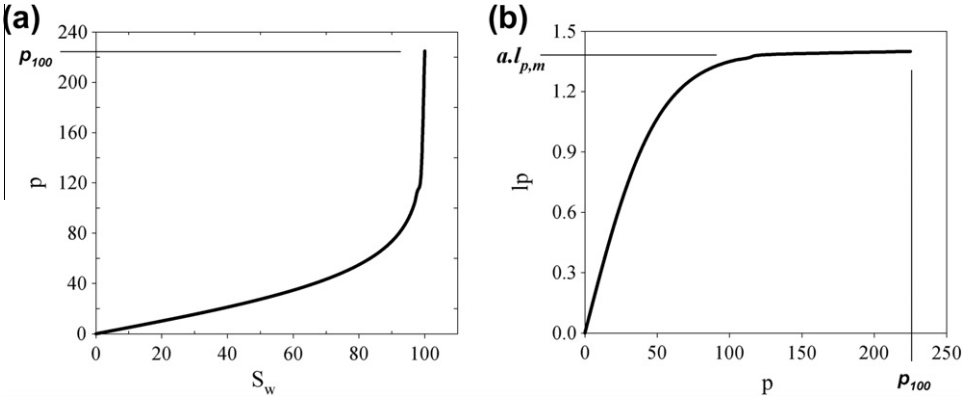

Fig. 2. (a) Saturation degree vs. pore pressure. (b) Internal characteristic length of porous phase vs. pore pressure.

obtained from Eq. (18), the governing Eq. (34) can be reformulated as

$$\int_\Omega \delta p\left(\frac{\Delta p}{M}+\mathbf{B}:\Delta\boldsymbol{\varepsilon}-(\mathbf{B}:\mathbf{m}_\sigma-\mathrm{m}_p)\Delta\lambda\right)\,\mathrm{d}\Omega = -\Delta t\int_\Omega \nabla\delta p\cdot\mathbf{k}\cdot\nabla p_j\,\mathrm{d}\Omega-\Delta t\int_\Omega\nabla\delta p\cdot\mathbf{k}\cdot\nabla\Delta p\,\mathrm{d}\Omega-\Delta t\times\int_{\partial\Omega}\delta p\mathbf{w}_{j+1}\cdot\mathbf{n}\,\mathrm{d}\partial\Omega \tag{38}$$

Following [19] the yield function Φ can be approximated with sufficient accuracy by means of a linear Taylor series around $(\boldsymbol{\sigma}_j,p_j,Q_{\alpha_j})$ as

$$\Phi(\boldsymbol{\sigma},p,Q_\alpha)|_{j+1}=\Phi(\boldsymbol{\sigma},p,Q_\alpha)|_j+\mathbf{n}_\sigma:\Delta\boldsymbol{\sigma}+\mathrm{n}_p\Delta p+\mathrm{n}_{Q_\alpha}\Delta Q_\alpha \tag{39}$$

When all state variables are spatially homogeneous it can be assumed that the dissipative stress gradient is negligible, then $\nabla Q_\alpha=0$, see [26,39–41].

From the additive decomposition of the dissipative stress in Eq. (10) follows

$$\dot{Q}_\alpha=\dot{Q}_\alpha^{loc}+\dot{Q}_\alpha^{nloc}=-H_\alpha^{loc}\mathrm{m}_{Q_\alpha}\dot{\lambda}+l_\alpha^2\mathbf{H}_\alpha^{nloc}\mathrm{m}_{Q_\alpha}\nabla^2\dot{\lambda} \tag{40}$$

by replacing Eqs. (19) and (40) in Eq. (39) the weak form of the yield condition is obtained

$$\int_\Omega\delta\lambda\;\Phi(\boldsymbol{\sigma},p,Q_\alpha)|_{j+1}\,\mathrm{d}\Omega=\int_\Omega\delta\lambda\;\Phi(\boldsymbol{\sigma},p,Q_\alpha)|_j\,\mathrm{d}\Omega+\int_\Omega\delta\lambda\,\mathbf{n}_\sigma:\mathbf{C}^0:\Delta\boldsymbol{\varepsilon}\,\mathrm{d}\Omega+\int_\Omega\delta\lambda\Big[(\mathrm{n}_p-\mathbf{n}_\sigma:\mathbf{B})\Delta p-\mathbf{n}_\sigma:\mathbf{C}^0:\mathbf{m}_\sigma\Delta\lambda+\mathrm{n}_{Q_\alpha}\left(-H_\alpha^{loc}\mathrm{m}_{Q_\alpha}\Delta\lambda+l_\alpha^2\mathbf{H}_\alpha^{nloc}\mathrm{m}_{Q_\alpha}\nabla^2\Delta\lambda\right)\Big]\mathrm{d}\Omega=0 \tag{41}$$

4.2. Galerkin discretization

This formulation was originally proposed by [11] for solid materials. As it can be observed in Eqs. (37), (38) and (41) at most first order derivatives of the displacement and pore pressure fields appear as well as second order derivative of the plastic multiplier. Therefore, displacement and pressure field discretizations require C_0-continuous shape functions that are indicated as $\mathbf{N}_u$ and $\mathbf{N}_p$, respectively. However, C_1-continuous shape functions, called $\mathbf{H}$, are required for the plastic multiplier discretization. Then, FE approximations can be expressed as

$$\mathbf{u}=\mathbf{N}_u\;\bar{\mathbf{u}} \tag{42}$$
$$p=\mathbf{N}_p\;\bar{p} \tag{43}$$
$$\lambda=\mathbf{H}\;\bar{\lambda} \tag{44}$$

where $\bar{\mathbf{u}}$, $\bar{p}$ and $\bar{\lambda}$ are the nodal displacement vector, the pore pressure and the plastic multiplier, respectively. Hence considering $\boldsymbol{\varepsilon}=\nabla^s\mathbf{u}=\nabla^s\mathbf{N}_u\;\bar{\mathbf{u}}=\overline{\mathbf{B}}\;\bar{\mathbf{u}}$ and replacing the above entities in Eqs. 37, 38 and 41 the following set of integral equations is obtained

$$\left\{\int_\Omega\delta\bar{\mathbf{u}}^T\overline{\mathbf{B}}^T:\mathbf{C}^0:\overline{\mathbf{B}}\,\mathrm{d}\Omega\right\}\Delta\bar{\mathbf{u}}-\left\{\int_\Omega\delta\bar{\mathbf{u}}^T\overline{\mathbf{B}}^T:\mathbf{B}\mathbf{N}_p\,\mathrm{d}\Omega\right\}\Delta\bar{p}-\left\{\int_\Omega\delta\bar{\mathbf{u}}^T\overline{\mathbf{B}}^T:\mathbf{C}^0:\mathbf{m}_\sigma\mathbf{H}\,\mathrm{d}\Omega\right\}\Delta\bar{\lambda}=\int_{\partial\Omega}\delta\bar{\mathbf{u}}^T\mathbf{N}_u^T\mathbf{t}_{j+1}\mathrm{d}\partial\Omega-\int_\Omega\delta\bar{\mathbf{u}}^T\overline{\mathbf{B}}^T:\boldsymbol{\sigma}_j\mathrm{d}\Omega \tag{45}$$

$$\left\{\int_\Omega\delta\bar{p}\;\mathbf{N}_p^T\mathbf{B}:\overline{\mathbf{B}}\,\mathrm{d}\Omega\right\}\Delta\bar{\mathbf{u}}+\left\{\int_\Omega\delta\bar{p}\left[\frac{\mathbf{N}_p^T\mathbf{N}_p}{M}+\Delta t(\nabla\mathbf{N}_p)^T\cdot\mathbf{k}\cdot\nabla\mathbf{N}_p\right]\mathrm{d}\Omega\right\}\Delta\bar{p}+\left\{\int_\Omega\delta\bar{p}\mathbf{N}_p^T[\mathrm{m}_p-\mathbf{B}:\mathbf{m}_\sigma]\mathbf{H}\,\mathrm{d}\Omega\right\}\Delta\bar{\lambda}=-\{\Delta t\int_\Omega\delta\bar{p}(\nabla\mathbf{N}_p)^T\cdot\mathbf{k}\cdot\nabla\mathbf{N}_p\,\mathrm{d}\Omega\}\bar{p}_j-\Delta t\int_{\partial\Omega}\delta\bar{p}\mathbf{N}_p^T\mathbf{w}_{j+1}\cdot\mathbf{n}\,\mathrm{d}\partial\Omega \tag{46}$$

$$\left\{\int_\Omega\delta\bar{\lambda}\mathbf{H}^T\mathbf{n}_\sigma:\mathbf{C}^0:\overline{\mathbf{B}}\,\mathrm{d}\Omega\right\}\Delta\bar{\mathbf{u}}+\left\{\int_\Omega\delta\bar{\lambda}\mathbf{H}^T[\mathrm{n}_p-\mathbf{n}_\sigma:\mathbf{B}]\mathbf{N}_p\,\mathrm{d}\Omega\right\}\Delta\bar{p}+\left\{-\int_\Omega\delta\bar{\lambda}\mathbf{H}^T\left[\mathbf{n}_\sigma:\mathbf{C}^0:\mathbf{m}_\sigma+\overline{H}_\alpha^{loc}\right]\mathbf{H}+l_\alpha^2\mathbf{H}^T\overline{\mathbf{H}}_\alpha^{nloc}\mathbf{P}\,\mathrm{d}\Omega\right\}\Delta\bar{\lambda}=-\int_\Omega\delta\bar{\lambda}\mathbf{H}^T\;\Phi(\boldsymbol{\sigma}_j,p_j,Q_{\alpha_j})\,\mathrm{d}\Omega \tag{47}$$

where

$$\nabla^2(\Delta\lambda)=\nabla^2(\mathbf{H})\Delta\bar{\lambda}=\mathbf{P}\Delta\bar{\lambda} \tag{48}$$
$$\overline{H}_\alpha^{loc}=\mathrm{n}_{Q_\alpha}H_\alpha^{loc}\mathrm{m}_{Q_\alpha} \tag{49}$$
$$\overline{\mathbf{H}}_\alpha^{nloc}=\mathrm{n}_{Q_\alpha}\mathbf{H}_\alpha^{nloc}\mathrm{m}_{Q_\alpha} \tag{50}$$

Eqs. (45)–(47) must hold for any admissible variation of $\delta\bar{\mathbf{u}}$, $\delta\bar{p}$ and $\delta\bar{\lambda}$. Thus, the algebraic equation in matrix form of the proposed FE for gradient-dependent poroplastic media can be expressed as

$$\begin{bmatrix}-\mathbf{K}_{ss} & \mathbf{Q}_{sp} & \mathbf{Q}_{s\lambda}\\ \mathbf{Q}_{ps} & \mathbf{K}_{pp}+\Delta t\mathbf{H}_{pp} & \mathbf{Q}_{p\lambda}\\ \mathbf{Q}_{\lambda s} & \mathbf{Q}_{\lambda p} & -\mathbf{K}_{\lambda\lambda}\end{bmatrix}\begin{bmatrix}\Delta\bar{\mathbf{u}}\\ \Delta\bar{p}\\ \Delta\bar{\lambda}\end{bmatrix}=\begin{bmatrix}\mathbf{F}_s^{int}-\mathbf{F}_s^{ext}\\ -\mathbf{F}_p\\ -\mathbf{F}_\lambda\end{bmatrix} \tag{51}$$

Submatrices of Eq. (51), presented in Appendix A, were obtained from Eqs. (45)–(47).

In Table 1, the solution algorithm of the BVP is summarized.

The main difference between this C_1-continuous FE formulation and the one based on C_0 continuity approximations for gradient plasticity proposed by [6,20] is the solution procedure. While present formulation requires only the solution of Eq. (51) the FE approaches proposed by the aforementioned authors require an additional global iteration to obtain the plastic multiplier.

Another meaningfully characteristic of present FE approach for gradient-poroplasticity as compared to standards classical plasticity related formulations is that the return mapping algorithm for the plastic multiplier is not longer required, since this state parameter is obtained from Eq. (51).

Table 1
Gradient-plasticity algorithm for C_1-continuous FE.

(1) Compute matrices of Eq. (51) according to Appendix A
(2) Solve the algebraic system of Eq. (51) in terms of the increments $\Delta\bar{\mathbf{u}}$, $\Delta\bar{p}$ and $\Delta\bar{\lambda}$
(3) Update primary variables $\Delta\bar{\mathbf{u}}_{j+1}=\Delta\bar{\mathbf{u}}_j+\Delta\bar{\mathbf{u}}$, $\Delta\bar{p}_{j+1}=\Delta\bar{p}_j+\Delta\bar{p}$ and $\Delta\bar{\lambda}_{j+1}=\Delta\bar{\lambda}_j+\Delta\bar{\lambda}$
(4) On each integration point compute:

$\Delta\boldsymbol{\varepsilon}_{j+1}=\overline{\mathbf{B}}\;\Delta\bar{\mathbf{u}}_{j+1}$
$\Delta\lambda_{j+1}=\mathbf{H}\;\Delta\bar{\lambda}_{j+1}$
$\nabla^2(\Delta\lambda_{j+1})=\mathbf{P}\;\Delta\bar{\lambda}_{j+1}$
$q_{\alpha_{j+1}}=q_{\alpha_0}+\mathrm{m}_{Q_\alpha}\Delta\lambda_{j+1}$
$\nabla^2q_{\alpha_{j+1}}=\nabla^2q_{\alpha_0}+\mathrm{m}_{Q_\alpha}\nabla^2(\Delta\lambda_{j+1})$
$\boldsymbol{\sigma}^t=\boldsymbol{\sigma}_0+\mathbf{C}^0:\Delta\boldsymbol{\varepsilon}_{j+1}-\mathbf{B}\mathbf{N}_p\Delta\bar{p}_{j+1}$
IF $\Phi(\boldsymbol{\sigma}^t,q_\alpha,\nabla^2q_\alpha)|_{j+1}>0$
$\quad\boldsymbol{\sigma}_{j+1}=\boldsymbol{\sigma}^t-\Delta\lambda_{j+1}\mathbf{C}^0:\mathbf{m}_\sigma$
ELSE
$\quad\boldsymbol{\sigma}_{j+1}=\boldsymbol{\sigma}^t$
END

(5) Check convergence criterion, i.e. balance between internal and external energy. If it is not achieved go to 1

4.3. FE stability and boundary conditions

In this section the stability requirements of the proposed FE are analyzed.

As previously discussed, the thermodynamically consistent gradient-plasticity formulation for porous media proposed by the authors [10] which is particularized here for saturated soils, involves the Laplacian of the plastic multiplier in its variational form. Therefore, C_1-continuous shape function are needed in order to appropriately describe the plastic multiplier field in the element domain as well as on its boundary.

Consolidation problems in saturated soils require the fulfilment of the Babuska–Brezzi condition [37,42] to avoid instabilities in their numerical solution procedures. This is particularly necessary when approaching the undrained limit state, where the permeability matrices turn zero. In this case, the system to be solved turns similar to those corresponding to incompressible elastic solids and, therefore, no real solution of Eq. (51) may arise. Nevertheless, if the undrained limit state can never be achieved the choice of finite element shape functions is wide.

In present formulation the isoparametric 8-node quadrilateral FE for 2D problems is adopted. This element was sufficiently tested in several problems regarding multiphasic fluid flow in porous media [36,37,42–46]. The Babuska–Brezzi condition is properly satisfied by considering shape functions for the displacement field $\mathbf{N}_u$ that are of higher order than the one considered for the pressure field $\mathbf{N}_p$. This FE was also extensively used in gradient-plasticity problems [19,47] related to non-porous materials with very accurate results. Actually, this type of FE behaves as the combination of three separated elements. On the one hand, two elements based on C_0 approximations for the displacements (eight-node FE) and the pore pressure (four-node FE), respectively. On the other hand, a four-nodes rectangular element with hermitian shape functions to approximate the plastic multiplier.

Fig. 3 shows proposed FE for porous media with the corresponding degrees of freedom of each element node. In Fig. 4 the Hermitian shape functions of element node 1 that are considered for the plastic multiplier interpolation are plotted.

The additional degrees of freedom in the proposed FE formulation for porous media require their corresponding boundary condi-

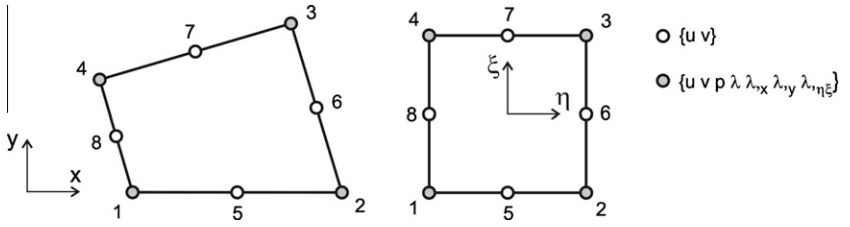

Fig. 3. 8-Node quadrilateral FE for gradient-plasticity in porous media.

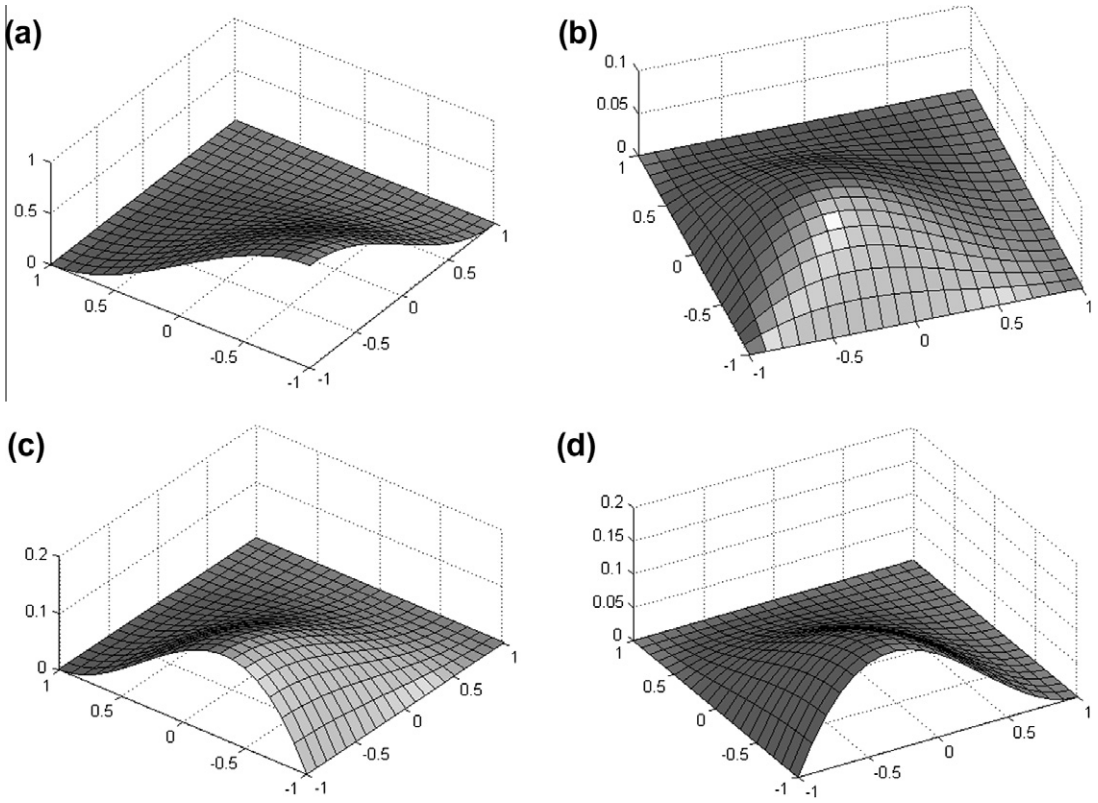

Fig. 4. Hermitian shape function for node 1: (a) for plastic multiplier λ, (b) for $\partial_{xy}\lambda$, (c) for $\partial_x\lambda$ and (d) for $\partial_y\lambda$.

tions. Following [48–51] we adopt Eq. (52) for the non-standard boundary condition. This is the natural and most appropriated choice, since the averaged strain measure itself cannot be constrained to zero on the boundary, in order to avoid the FE stiffness matrix to turn singular.

$$\partial_n \lambda = 0 \quad \text{and} \quad \partial_{nm} \lambda = 0 \tag{52}$$

where n and m denote the normal and tangential directions to the model boundary, respectively.

5. Numerical result

In this section numerical evaluations of the proposed FE formulation for gradient-based poroplasticity are presented. The main objective is to evaluate the robustness of the numerical tools and the predictive capabilities of the constitutive theory proposed by the authors [10] when combined with the non-associated Cam Clay model as described in Section 3. The influence of the gradient characteristic length on the ductility in post-peak regime is also evaluated.

A plane strain specimen under biaxial state of loading is consider in order to evaluate localized failure mode of porous media. Fig. 5 shows geometry and displacements boundary conditions of the specimen while material parameters are given in Table 2. The dimensions assumed are $B = 60$ mm and $H = 120$ mm. Drained conditions for the porous phase are also considered in this numerical example.

To create an inhomogeneous loading state and to induce localized failure mode a weakened region of $d = 10$ mm in the bottom left-hand corner of the specimen was considered by assigning an initial preconsolidation pressure which is 10% reduced as compared to the material outsides this weakened zone (see Fig. 5).

The supplementary boundary conditions considered in this analysis due to the additional degrees of freedom of the problem are: $\partial_x \lambda = 0$ on left and right boundaries, $\partial_y \lambda = 0$ on top and bottom boundaries, and $\partial_{xy} \lambda = 0$ along the whole boundary.

Four different meshes (three structured, Fig. 6a, c and d, and one non-structured, Fig. 6b) were considered in this analysis in order to evaluate the FE mesh size and orientation sensitivities of the numerical predictions. Therefore, the characteristic length of the saturated soil is assumed constant $l_s = 3.5$ mm. As can be observed in Fig. 6 the localization band width remains practically constant in all meshes when the gradient length is set constant, $w = 2\pi l_s$ -

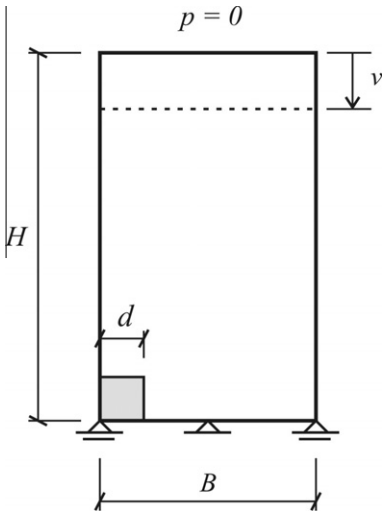

Fig. 5. Geometry and boundary conditions.

Table 2
Soil material parameters.

Material parameters	Value
CSL slope, M	1.00
Preconsolidation pressure, p_{co}	100.00 MPa
Initial porosity, ϕ_0	0.4
Bulk compressibility coefficient, K_0	1000.00
Solid compressibility coefficient, K_s	1500.00
Fluid compressibility coefficient, K_{fl}	500.00
Biot coefficient, $b = 1 - K_0/K_s$	0.33
Young module, E	20000.0 MPa
Poisson ratio, v	0.2
Local hardening/softening module, $H_s^{loc} = H_p^{loc}$	$-0.1 * E$

$\cong 20$ mm. This result demonstrates the capability of the proposed FE formulation to capture the considered non-local effects through the additional degrees of freedom.

The mesh objectivity or softening regularization capabilities of the numerical predictions can also be demonstrated by observing the good agreement between the load–displacement curves for the four different meshes in Fig. 7. Also the stress path of the material point where the plastic process initiates is illustrated in Fig. 8.

A second set of analyses of this test was performed with three different gradient characteristic lengths and totally drained conditions. Only the 12×24 regular mesh of Fig. 6 was used in this case. Fig. 9 shows FE predictions considering $l_s = 3.0$ mm, $l_s = 3.5$ mm and $l_s = 4$ mm, being its localization band width $w \cong 15$ mm, $w \cong 20$ mm and $w \cong 25$ mm, respectively. It can be clearly observed in these results that the proposed FE formulation is able to reproduce the model sensitivity to the characteristic length. A significant improvement of the ductility takes place under increasing l_s.

The equivalent plastic strain distribution at residual strength of the numerical analysis can be observed in Fig. 10. The increment of the plastic dissipation zone with increasing internal characteristic length can be clearly recognized.

The third set of analysis was carried out varying the confinement pressure in the soil specimen. As explained before, the internal characteristic length of the solid skeleton l_s is a function of the acting confining pressure (see Fig. 1).

In this third set of analysis three different confining pressure were applied, 5, 13 and 21 MPa, and the extreme value of the internal characteristic length of the solid phase is $l_{s,\,m} = 7$ mm. Fig. 11 shows the transition from quasi-brittle to ductile behavior of the considered soil specimen. Also, for a better understanding of the results in Fig. 11, the stress path of the material point where the plastic process initiates is depicted in Fig. 12.

Finally, a numerical example of the previous test was performed considering three different levels of initial pore pressure: $p = 20$, $p = 40$ and $p = 60$. Also the coefficients of the Eq. (32) are $a = 1.0$, $b = 0.02$ and the extreme value of the internal characteristic length of the porous phase is $l_{p,m} = 7$ mm. In Fig. 13 the equivalent plastic strain in the soil specimen is depicted. As in previous set of analysis, it can be easily recognize in this case the transition from ductile to brittle failure mode as the pore pressure level reduces.

6. Conclusions

In this paper a thermodynamically consistent finite element formulation for gradient-based poroplasticity with non-local effect restricted to the internal variables was proposed. The element formulation includes C_0 continuous approximations for both the pore pressure and the displacements fields, while a C_1-continuous interpolation function for the internal variable. These Hermitian functions need to be considered to approximate the gradient fields

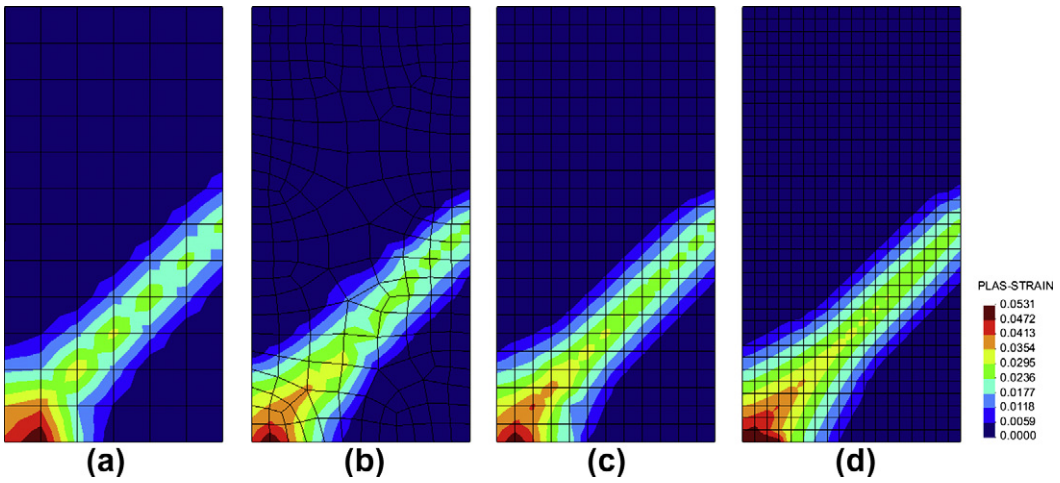

Fig. 6. FE mesh dependence.

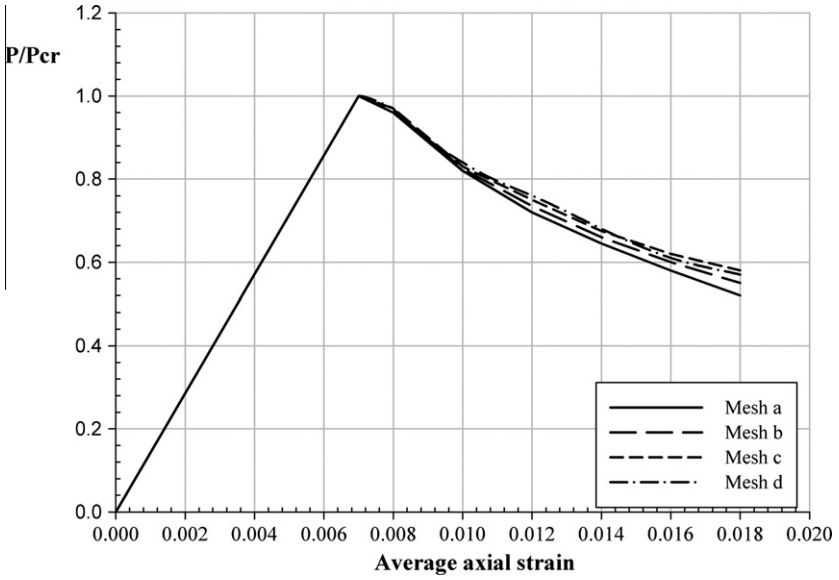

Fig. 7. Normalized load–displacement curves for different mesh size and orientation.

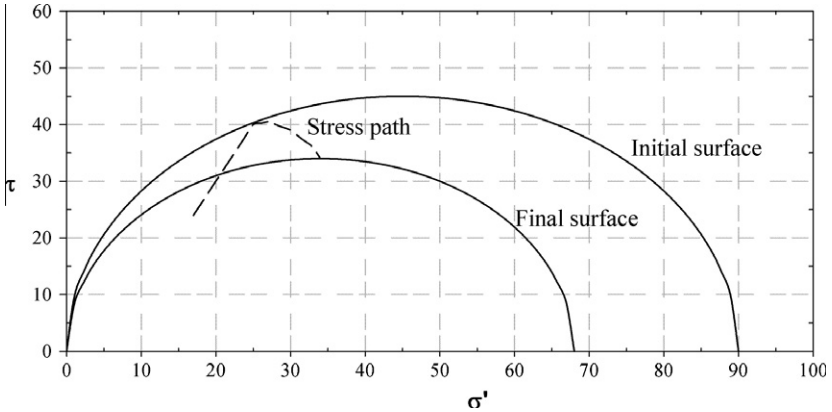

Fig. 8. Stress path and yield surface evolution.

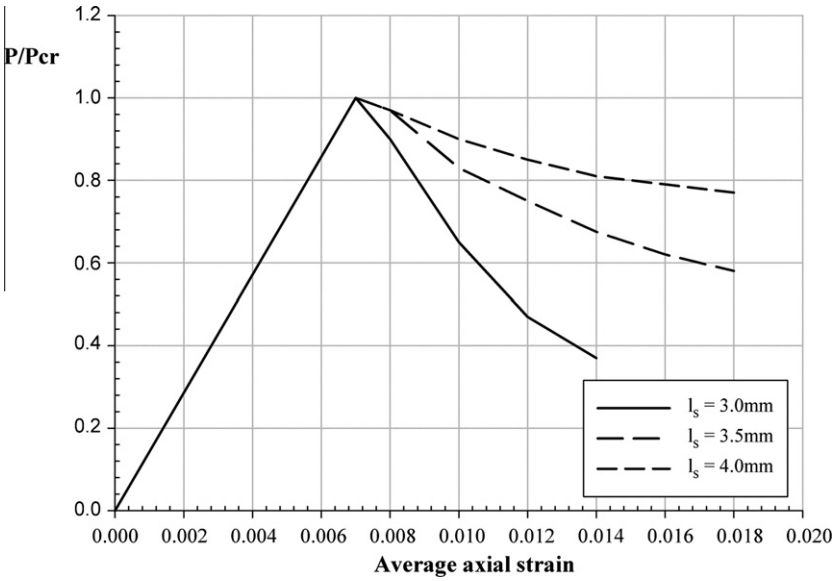

Fig. 9. Normalized load–displacement curve for variable l_s.

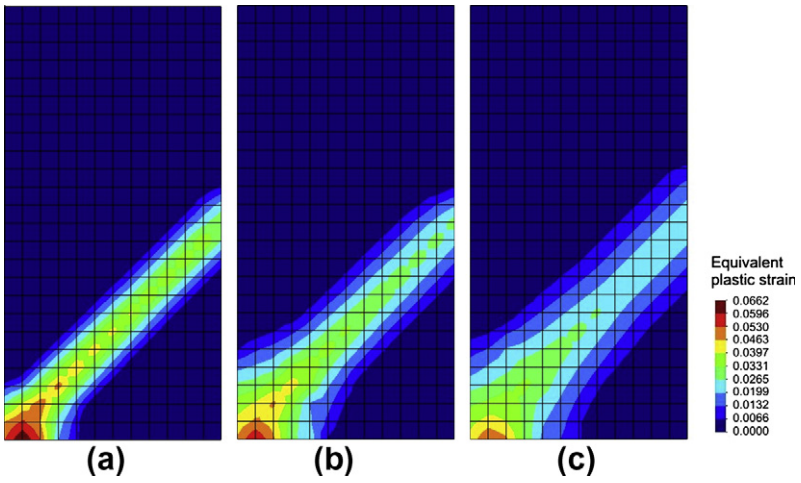

Fig. 10. Equivalent plastic strain for different constant values of l_s, (a) l_s = 3.0 mm, (b) l_s = 3.5 mm and (c) l_s = 4 mm.

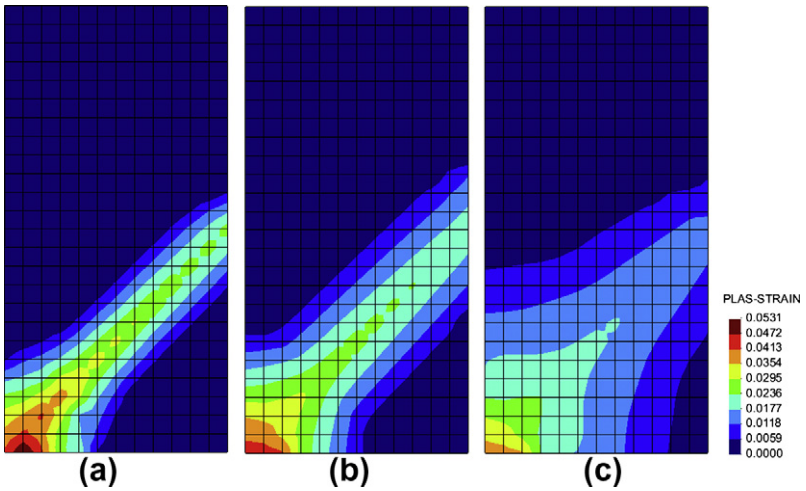

Fig. 11. Equivalent plastic strain considering l_s as a function of confining pressure, (a) 5, (b) 13 and (c) 21 MPa.

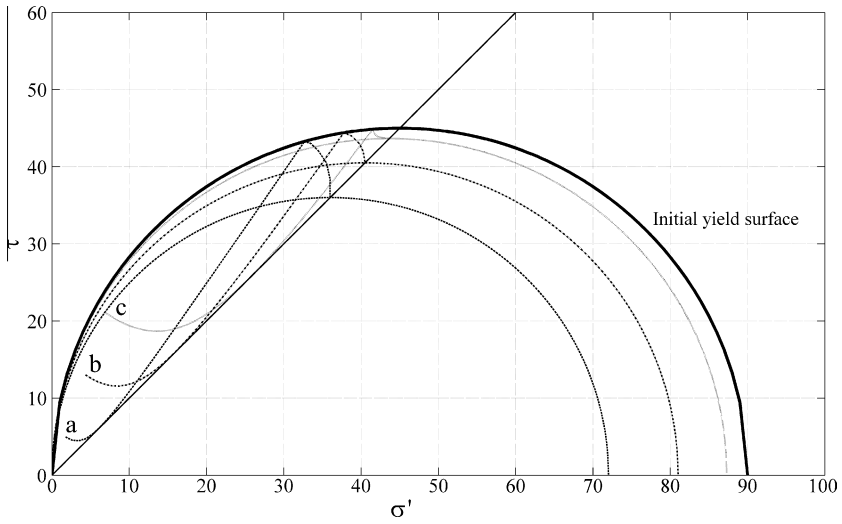

Fig. 12. Stress path and yield surface evolution corresponding to three confining pressures, (a) 5, (b) 13 and (c) 21 MPa.

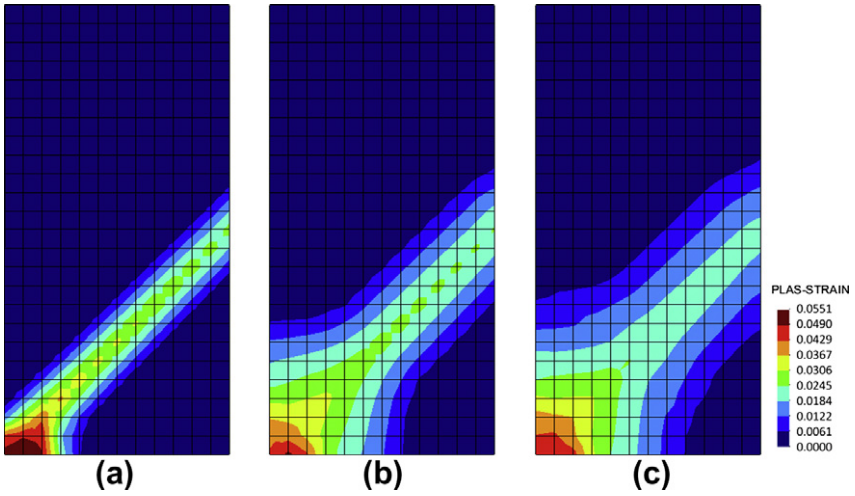

Fig. 13. Equivalent plastic strain considering l_p as a function of pore pressure, (a) $p = 20$, (b) $p = 40$ and (c) $p = 60$.

that are included in the variational problem due to the non-local gradient formulation assumed at the constitutive level.

The numerical analyses in this work demonstrate the capabilities of the proposed FE formulation to reproduce failure behaviors of saturated porous media under different boundary conditions and material features. Particularly, it is shown that the proposed FE is able to reproduce model sensitivity regarding the gradient characteristic length while assuring mesh objectivity.

Appendix A. Matrix expressions of Eq. (51)

The matrix expressions of the FE stiffness matrix for gradient-plasticity Eq. (51) are

$$\mathbf{K}_{ss} = \int_{\Omega} \overline{\mathbf{B}}^{T} : \mathbf{C}^{0} : \overline{\mathbf{B}}\ \mathrm{d}\Omega \tag{A.1}$$

$$\mathbf{K}_{pp} = \int_{\Omega} \frac{\mathbf{N}_p^{T}\mathbf{N}_p}{M}\mathrm{d}\Omega \tag{A.2}$$

$$\mathbf{K}_{\lambda\lambda} = \int_{\Omega} \mathbf{H}^{T}\left[\mathbf{n}_{\sigma} : \mathbf{C}^{0} : \mathbf{m}_{\sigma} + \overline{H}_{\alpha}^{loc}\right]\mathbf{H} + l_{\alpha}^{2}\mathbf{H}^{T}\overline{\mathbf{H}}_{\alpha}^{nloc}\mathbf{P}\ \mathrm{d}\Omega \tag{A.3}$$

$$\mathbf{H}_{pp} = \int_{\Omega} (\nabla \mathbf{N}_p)^{T} \cdot \mathbf{k} \cdot \nabla \mathbf{N}_p \mathrm{d}\Omega \tag{A.4}$$

$$\mathbf{Q}_{sp} = \int_{\Omega} \overline{\mathbf{B}}^{T} : \mathbf{B}\mathbf{N}_p\ \mathrm{d}\Omega \tag{A.5}$$

$$\mathbf{Q}_{ps} = \int_{\Omega} \mathbf{N}_p^{T}\mathbf{B} : \overline{\mathbf{B}}\ \mathrm{d}\Omega \tag{A.6}$$

$$\mathbf{Q}_{s\lambda} = \int_{\Omega} \overline{\mathbf{B}}^{T} : \mathbf{C}^{0} : \mathbf{m}_{\sigma}\mathbf{H}\ \mathrm{d}\Omega \tag{A.7}$$

$$\mathbf{Q}_{\lambda s} = \int_{\Omega} \mathbf{H}^{T}\mathbf{n}_{\sigma} : \mathbf{C}^{0} : \overline{\mathbf{B}}\ \mathrm{d}\Omega \tag{A.8}$$

$$\mathbf{Q}_{p\lambda} = \int_{\Omega} \mathbf{N}_p^{T}[\mathrm{m}_p - \mathbf{B} : \mathbf{m}_{\sigma}]\mathbf{H}\ \mathrm{d}\Omega \tag{A.9}$$

$$\mathbf{Q}_{\lambda p} = \int_{\Omega} \mathbf{H}^{T}[\mathrm{n}_p - \mathbf{n}_{\sigma} : \mathbf{B}]\mathbf{N}_p\ \mathrm{d}\Omega \tag{A.10}$$

$$\mathbf{F}_{s}^{int} = \int_{\Omega} \overline{\mathbf{B}}^{T} : \boldsymbol{\sigma}_j \mathrm{d}\Omega \tag{A.11}$$

$$\mathbf{F}_{s}^{ext} = \int_{\partial\Omega} \mathbf{N}_u^{T}\mathbf{t}_{j+1}\mathrm{d}\partial\Omega \tag{A.12}$$

$$\mathbf{F}_{p} = \Delta t\mathbf{H}_{pp}\bar{p}_j + \Delta t\int_{\partial\Omega} \mathbf{N}_p^{T}\mathbf{w}_{j+1} \cdot \mathbf{n}\ \mathrm{d}\partial\Omega \tag{A.13}$$

$$\mathbf{F}_{\lambda} = \int_{\Omega} \mathbf{H}^{T}\ \Phi(\boldsymbol{\sigma}_j, p_j, \mathrm{Q}_{\alpha_j})\ \mathrm{d}\Omega \tag{A.14}$$

References

[1] Vardoulakis I, Aifantis EC. A gradient flow theory of plasticity for granular materials. Acta Mech 1991;87(3–4):197–217.
[2] Peerlings R, de Borst R, Brekelmans W, Geers M. Gradient-enhanced damage modelling of concrete fracture. Mech Cohes – Frict Mater 1998;3(4):323–42.
[3] Comi C. Non-local model with tension and compression damage mechanisms. Eur J Mech A – Solid 2001;20(1):1–22.
[4] Pan Y, Wang X, Li Z. Analysis of the strain softening size effect for rock specimens based on shear strain gradient plasticity theory. Int J Rock Mech Min 2002;39(6):801–5.
[5] Simone A, Wells GN, Sluys LJ. From continuous to discontinuous failure in a gradient-enhanced continuum damage model. Comput Methods Appl Mech 2003;192(41–42):4581–607.
[6] Vrech S, Etse G. FE approach for thermodynamically consistent gradient-dependent plasticity. Latin Am Appl Res 2007;37:127–32.
[7] Fredriksson P, Gudmundson P, Mikkelsen LP. Finite element implementation and numerical issues of strain gradient plasticity with application to metal matrix composites. Int J Solids Struct 2009;46(22–23):3977–87.
[8] Sabatini PJ, Finno RJ. Effect of consolidation on strain localization of soft clays. Comput Geotech 1996;18(4):311–39.
[9] Kristensson O, Ahadi A. Numerical study of localization in soil systems. Comput Geotech 2005;32(8):600–12.
[10] Mroginski JL, Etse G, Vrech SM. A thermodynamical gradient theory for deformation and strain localization of porous media. Int J Plast 2011;27: 620–34.
[11] de Borst R, Mühlhaus HB. Gradient-dependent plasticity: formulation and algorithmic aspects. Int J Numer Methods Eng 1992;35:521–39.
[12] de Borst R, Pamin J. Gradient plasticity in numerical simulation of concrete cracking. Eur J Mech A – Solid 1996;15(2):295–320.
[13] Xikui LI, Cescotto S. Finite element method for gradient plasticity at large strains. Int J Numer Methods Eng 1996;39(4):619–33.
[14] de Borst R, Pamin J. Some novel developments in finite element procedures for gradient-dependent plasticity. Int J Numer Methods Eng 1996;39(14): 2477–505.
[15] Ramaswamy S, Aravas N. Finite element implementation of gradient plasticity models part I: gradient-dependent yield functions. Comput Methods Appl Mech 1998;163(1–4):11–32.
[16] Shu JY, King WE, Fleck NA. Finite elements for materials with strain gradient effects. Int J Numer Methods Eng 1999;44(3):373–91.
[17] Wang ZM, Zhu XA, Tsai CT, Tham CL, Beraun JE. Hybrid-conventional finite element for gradient-dependent plasticity. Finite Elem Anal Des 2004;40(15): 2085–100.
[18] Swaddiwudhipong S, Hua J, Tho KK, Liu ZS. C_0 solid elements for materials with strain gradient effects. Int J Numer Methods Eng 2005;64(10):1400–14.
[19] Pamin J. Gradient-dependent plasticity in numerical simulation of localization phenomena. Ph.D. thesis, TU-Delft, The Netherlands; 1994.
[20] Svedberg T, Runesson K. An algorithm for gradient-regularized plasticity coupled to damage based on a dual mixed fe-formulation. Comput Methods Appl Mech 1998;161:49–65.
[21] Stankiewicz A, Pamin J. Gradient-enhanced cam-clay model in simulation of strain localization in soil. Found Civil Environ Eng 2006;7:293–318.
[22] Pamin J, Stankiewicz A. Numerical simulation of instabilities in one- and two-phase soil model based on Cam-clay plasticity. Tech Trans 2008;20:81–91 [series environmental engineering 3-S/2008].
[23] Stankiewicz A, Pamin J. Finite element analysis of fluid influence on instabilities in two-phase cam-clay plasticity model. Comput Assist Mech Eng Sci 2006;13(4):669–82.
[24] Simo J, Miehe C. Associative coupled thermoplasticity at finite strains: formulation, numerical analysis and implementation. Comput Methods Appl Mech 1992;98(1):41–104.
[25] Coussy O. Mechanics of porous continua. John Wiley & Sons; 1995.
[26] Svedberg T, Runesson K. A thermodynamically consistent theory of gradient-regularized plasticity coupled to damage. Int J Plast 1997;13(6–7):669–96.
[27] Vrech SM, Etse G. Gradient and fracture energy-based plasticity theory for quasi-brittle materials like concrete. Comput Methods Appl Mech 2009;199(1–4):136–47.
[28] Svedberg T. On the modelling and numerics of gradient-regularized plasticity coupled to damage. Ph.D. thesis, Chalmers University of Technology, Gn++teborg, Sweden; 1999.
[29] Vrech S, Etse G. Geometrical localization analysis of gradient-dependent parabolic Drucker–Prager elastoplasticity. Int J Plast 2005;22(5):943–64.
[30] Roscoe K, Burland J. On the generalized stress–strain behaviour of wet clay. In: Heyman J, Leckie FA, editors. Engineering plasticity. Cambridge University Press; 1968.
[31] Alonso EE, Gens A, Josa A. A constitutive model for partially saturated soils. Geotechnique 1990;40(3):405–30.
[32] Bolzon G, Schrefler B, Zienkiewicz O. Elastoplastic soil constitutive laws generalized to partially saturated states. Geotechnique 1996;46(2): 279–n++289.
[33] Pedroso DM, Farias MM. Extended barcelona basic model for unsaturated soils under cyclic loadings. Comput Geotech 2011;38(5):731–40.
[34] Balmaceda A. Compacted soils, a theoretical and experimental study (in spanish). Tesis doctoral, Universidad Politn++cnica de Catalunya; 1991.
[35] Fredlund DG, Xing A. Equations for the soil–water characteristic curve. Can Geotech J 1994;31:521–32.
[36] Lewis RW, Schrefler BA. The finite element method in the static and dynamic deformation and consolidation of porous media. John Wiley & Sons; 1998.
[37] Mroginski JL, Di Rado HA, Beneyto PA, Awruch AM. A finite element approach for multiphase fluid flow in porous media. Math Comput Simul 2010;81: 76–91.
[38] Schreyer-Bennethum L. Theory of flow and deformation of swelling porous materials at the macroscale. Comput Geotech 2007;34(4):267–78.
[39] Vrech SM, Etse G. Discontinuous bifurcation analysis in fracture energy-based gradient plasticity for concrete. Int J Solids Struct 2012;49(10):1294–303.
[40] Ekh M, Grymer M, Runesson K, Svedberg T. Gradient crystal plasticity as part of the computational modelling of polycrystals. Int J Numer Methods Eng 2007;72(2):197–220.
[41] Nguyen QS, Andrieux S. The non-local generalized standard approach: a consistent gradient theory. Compt Rendus – Mec 2005;333(2):139–45.
[42] Schrefler BA, Pesavento F. Multiphase flow in deforming porous material. Comput Geotech 2004;31:237–50.
[43] Gawin D, Baggio P, Schrefler BA. Coupled heat water and gas flow in deformable porous media. Int J Numer Methods Fl 1995;20:969–87.
[44] Khalili N, Loret B. An elasto-plastic model for non-isothermal analysis of flow and deformation in unsaturated porous media: formulation. Int J Solids Struct 2001;38(46–47):8305–30.
[45] Pesavento F, Gawin D, Schrefler BA. Modeling cementitious materials as multiphase porous media: theoretical framework and applications. Acta Mech 2008;201(1–4):313–39.
[46] Di Rado HA, Beneyto PA, Mroginski JL, Awruch AM. Influence of the saturation–suction relationship in the formulation of non-saturated soils consolidation models. Math Comput Model 2009;49(5–6):1058–70.
[47] Dorgan RJ. A nonlocal model for coupled damage-plasticity incorporating gradients of internal state variables at multiscales. Ph.D. thesis, Louisiana State University; 2006.
[48] Pamin J, Askes H, de Borst R. Two gradient plasticity theories discretized with the element-free Galerkin method. Comput Methods Appl Mech 2003;192: 2377n++–2403.
[49] Poh LH, Swaddiwudhipong S. Over-nonlocal gradient enhanced plastic-damage model for concrete. Int J Solids Struct 2009;46:4369–78.
[50] Peerlings R, de Borst R, Brekelmans W, Vree J. Gradient-enhanced damage for quasi-brittle materials. Int J Numer Methods Eng 1996;39:3391–403.
[51] Geers M, de Borst R, Brekelmans W, Peerlings R. Strain-based transient-gradient damage model for failure analysis. Comput Methods Appl Mech 1998;160(1–2):133–53.